# Mass Determination in SUSY-like Events with Missing Energy

Jack Gunion
U.C. Davis

Collaborators: Hsin-Chia Cheng, Zhenyu Han, Guido Marandella, Bob McElrath

Based on arXiv:0707.0030 and ongoing work.

EPS and SUSY, July 2007

# Motivations for an invisible particle below the TeV Scale

1. To solve the Higgs boson mass hierarchy problem there must be new particles below the TeV scale.

2. Sub-TeV new physics avoids precision electroweak constraints most easily if there is a new discrete symmetry that requires that they couple in pairs to the SM particles (especially, the $W$ and $Z$).

3. The lightest such new particle will then be stable and could explain the observed dark matter in the universe.

4. In many models the correct dark matter density can be obtained and it will have evaded observational contraints (dark matter detection, ....) if this new particle is weakly interacting, $\longrightarrow$ WIMP

   $\Rightarrow$ **2** such particles (call them $N$) per LHC event that lead to variable and partially balancing missing momentum in each event.

## Popular Candidate Models

- **SUSY with $R$-parity conservation.**

  **The lightest supersymmetric particle (LSP) is likely to be a neutralino, which is a good WIMP candidate.**

- **Little Higgs Models with $T$-parity: lightest $T$-odd particle is a good WIMP.**

- **Universal Extra Dimensions: lightest KK mode (e.g. first excited 'photon') is a good WIMP.**

- **Models with warped unification with $Z_3$ parity, ...**

**Given the probable ILC time scales, the big question is if the LHC alone will be able to measure the properties of the WIMP candidate and its higher mass cousins that decay to it.**

**A very crucial part of the answer involves the accuracy with which mass scales can be determined at the LHC in the presence of missing energy!**

**The problem: In general, if there is a pair of invisible particles, then there is not enough information to reconstruct the kinematics of each event** *on an event-by-event basis*.

- **Mass scales will be important not only for the dark matter issue but also for the LHC inverse problem: Can we use LHC data to determine the fundamental Lagrangian parameters?**
  **And, can we do so with sufficient accuracy as to allow a meaningful extrapolation to the GUT scale?**
  **The general picture:**

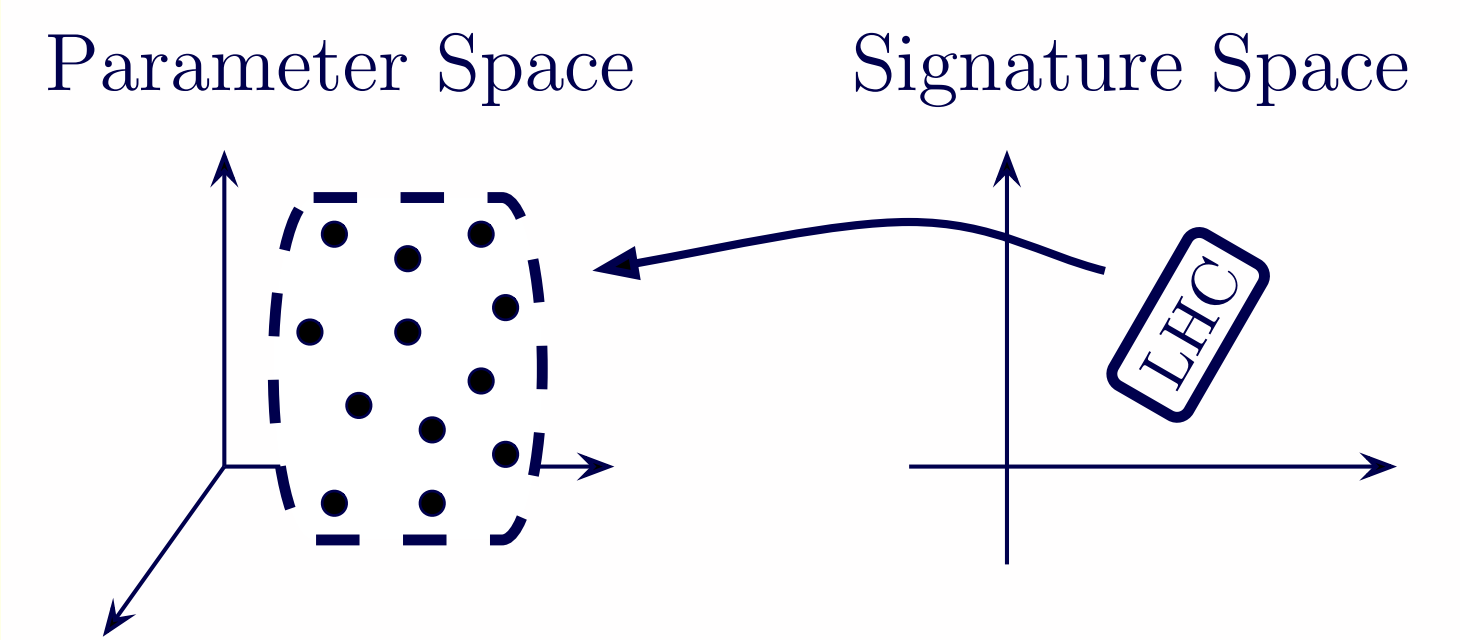


**Figure 1:** *The likely LHC situation. N. Arkani-Hamed, G. L. Kane, J. Thaler and L. T. Wang, JHEP* **0608**, *070 (2006) [arXiv:hep-ph/0512190].*

**The picture is particularly bad if the LHC will have a hard time determining the absolute mass scale.**

**As an example of the difficulties encountered, let us consider the mSUGRA SPS1a' point. It gives a spectrum of the following type:**

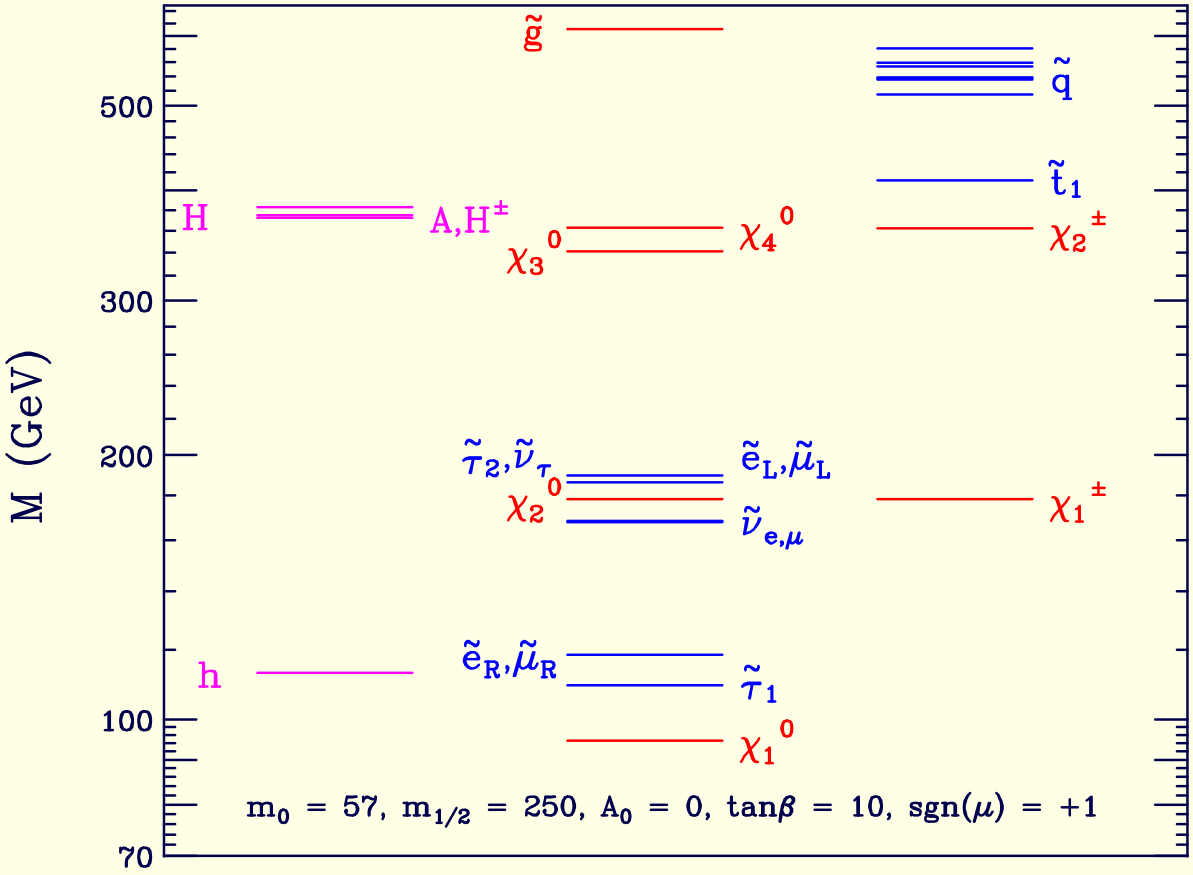


**Figure 2:** *Mass spectra of an SPS1a'-like point.*

**Using lepton spectrum edges and the like, one gets quite a bit of information about the spectrum, but a good determination of the overall mass scale is**

**elusive. $m_{\widetilde{\chi}_1^0}$ sets the overall scale.**

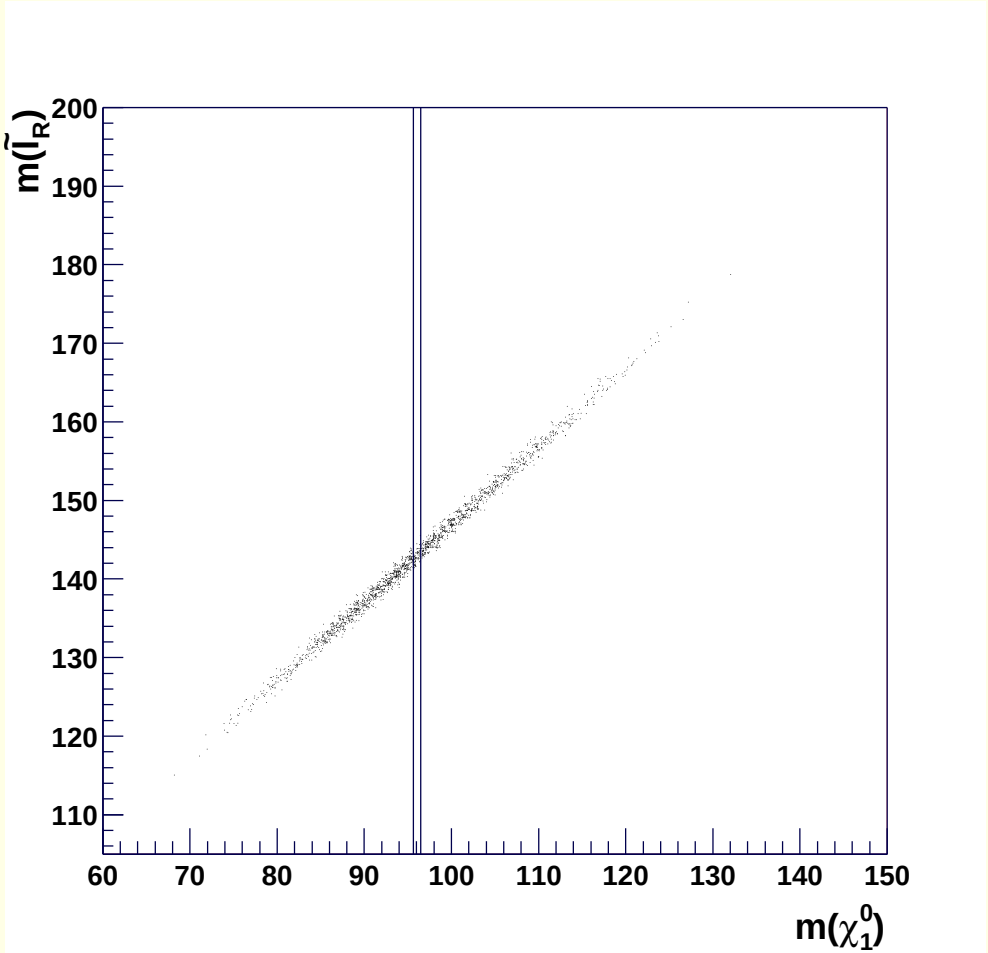


**Figure 3:** *Sample mass correlation plot. Dots: LHC alone; Vertical band* $= \pm 2\sigma$ *for ILC data. G. Weiglein et al. [LHC/LC Study Group], Phys. Rept.* **426**, *47 (2006) [arXiv:hep-ph/0410364]. Note: These results are for the SPS1a' 'dot'.*

**How does such LHC accuracy compare to what is needed?**

**a) A precision calculation of the dark matter primarily needs accurate masses (couplings being fixed by supersymmetry). The ILC measures $m_{\widetilde{\chi}_1^0}$ and other masses to within $\Delta m_{\widetilde{\chi}_1^0} \sim \pm 3$ GeV. Could we possibly reach this level at the LHC?**

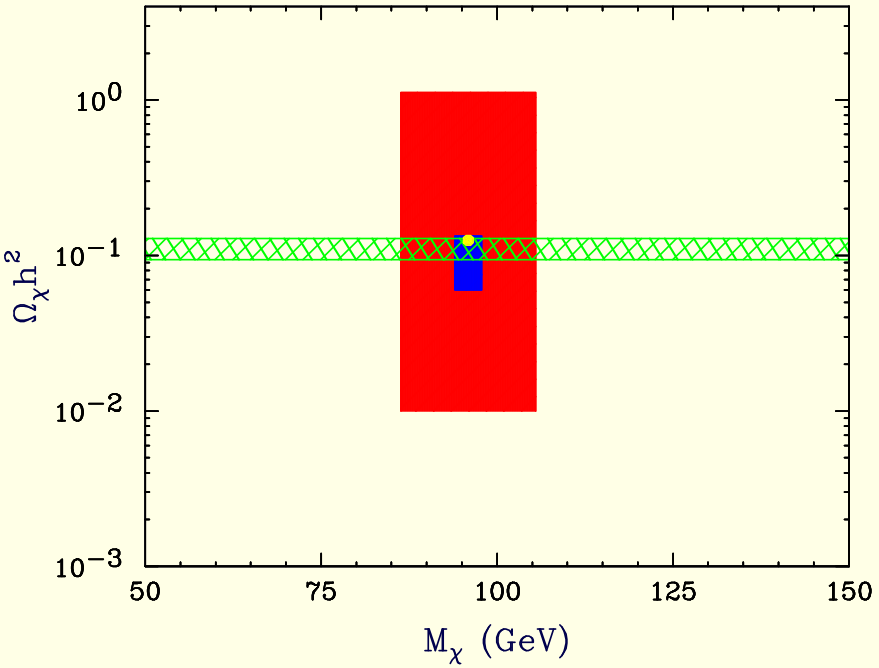


**Figure 4:** *Accuracy of WMAP (horizontal green shaded region), LHC (outer red rectangle) and ILC (inner blue rectangle) in determining $m_{\widetilde{\chi}_1^0}$, the mass of the lightest neutralino, and its relic density $\Omega_\chi h^2$. LHC is assumed to get 10% accuracy on absolute $m_{\widetilde{\chi}_1^0}, m_{\widetilde{\chi}_2^0}, m_{\widetilde{\chi}_1^\pm}$ masses = optimistic using usual techniques. The yellow dot denotes the actual values of $m_{\widetilde{\chi}_1^0}$ and $\Omega_\chi h^2$ for point B'. A. Birkedal, et al.hep-ph/0507214*

**b) Precision mass measurement are needed to meaningfully assess GUT scale boundary conditions.**

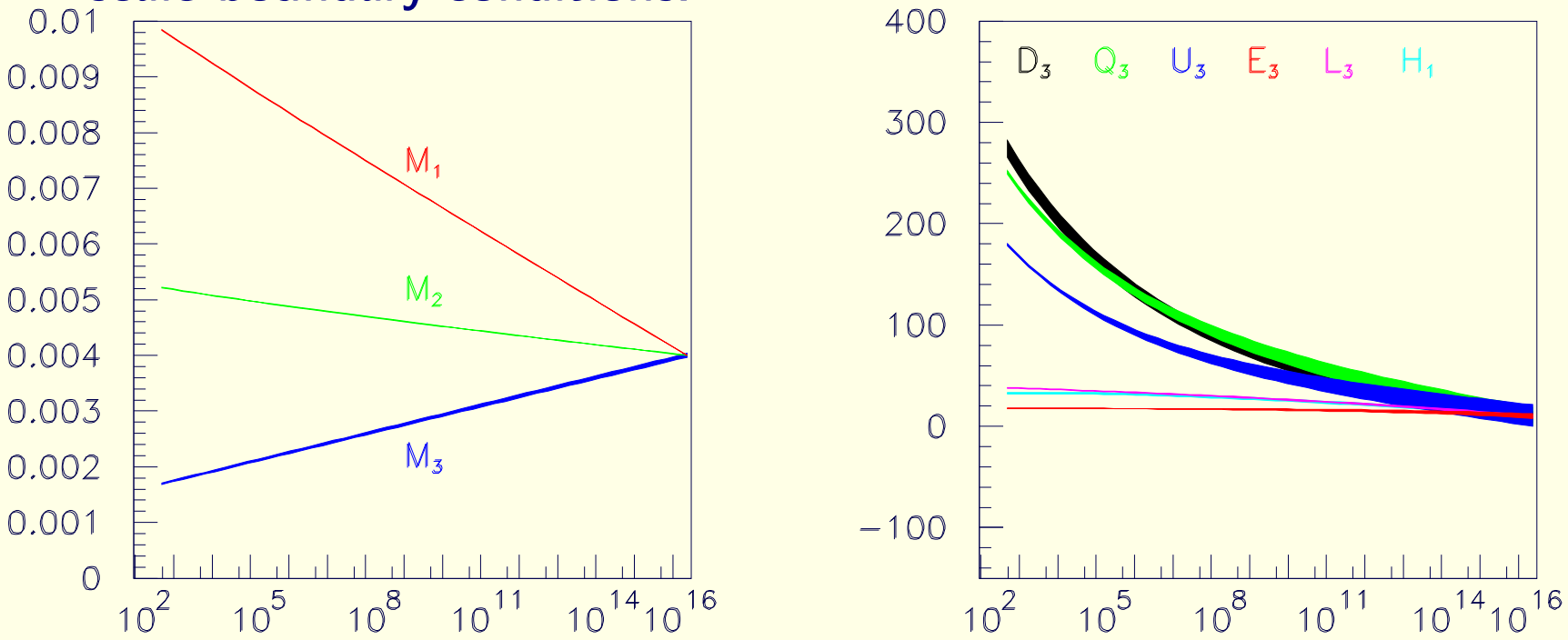


**Figure 5:** *Evolution to the GUT scale using LHC + ILC1000 measurements. On the left,* $1/M_i$ *[GeV*$^{-1}$*] is plotted vs.* $Q$( GeV). *On the right,* $M^2_{\tilde{j}}$ *[*$10^3$ *GeV*$^2$*] for 3rd soft masses squared are plotted vs.* $Q$( GeV).

**Differences between sparticle masses are determined at the LHC, but, will it require the ILC (e.g. via threshold scans) to get the absolute mass scales.**

**We must work to get absolute masses with the required accuracy using LHC data alone.**

# Basic Constraint Counting

## One chain examples

1. The "marginal" case is $3$ visible particles (or combinations of particles) with $3$ on-shell resonances involved and $1$ final invisible particle:

$$Z \to Y v_1 \to X v_2 v_1 \to N v_3 v_2 v_1 \tag{1}$$

   For this case, after $n$ events, the number of unknowns is $4$ masses and $4n$ $4$-momenta of the final invisible particle ($N$).

   The number of on-shell constraints from requiring given $Z, Y, X, N$ masses in each event is $4n$.

   Thus, the number of unknowns is always $4 + 4n - 4n = 4$ (the masses) no matter how many events.

2. For $4$ visible particles with $4$ on-shell resonances and the final $N$, after $n$ events there are $5 + 4n$ unknowns and $5n$ constraints, implying equality

when $n = 5$. So, if there were no combinatoric / resolution issues, $n = 5$ events would allow you to solve for the $5$ masses aside from discrete quartic equation solution ambiguities.

## Two chain examples

1. The "marginal" case here is just two visible particles per chain: $Y \to Xv_1 \to Nv_2v_1$.

   If we assume equal masses on the two chains, then there are $3$ unknown masses, including $m_N$.

   For each event, there are the two $4$-momenta of the two final $N$'s, but we know the sum of their transverse momenta from balancing against the visible particle transverse momenta, implying $6$ unknown momenta components per event.

   After $n$ events, the number of unknowns is then $3 + 6n$.

   The number of constraints is $6n$ (since we assume on-shell masses on both chains.)

   Thus, no matter how many events, we always have the $3$ unknown mass parameters that cannot be absolutely solved for.

Note that by considering both chains, we are at the marginal situation with just $2$ visible particles and $2$ on-shell resonances plus the $1$ final invisible particle, as opposed to the one-chain case where marginality required $3$ visible particles, corresponding to $3$ on-shell resonances plus $1$ invisible particle.

2. The first non-marginal case is clearly $3$ visible particles *per chain*, corresponding to $3 + 1 = 4$ unknown masses.

   In this case, after $n$ events we have $4 + 6n$ unknowns and $8n$ on-shell constraints (recall we have two chains each of which has four mass constraints) implying solution (subject to discrete ambiguities) when $4 + 6n - 8n = 0 \Rightarrow n = 2$.

   Again, there is a reduction in the number of on-shell resonances and associated visible particles that are needed to get discrete solutions, as compared to considering a single chain.

A significant problem with both the $1$-chain and $2$-chain approaches is combinatorics.

For example, for the decay chain $\widetilde{q} \to q\widetilde{\chi}_2^0 \to q\mu\widetilde{\mu}_R \to q\mu\mu\widetilde{\chi}_1^0$ in $\widetilde{q}\widetilde{q}$ production, in each event there would be $2!$ ways to place the $q$'s and

$4 \times 2 \times 2$ ways to place the $\mu$'s (noting that each chain has to have one $\mu^+$ and one $\mu^-$, but we don't know which comes first.) The net is $2 \times 16 = 32$ ways of placing particles.

If there are additional jets from ISR and / or from $\widetilde{g}\widetilde{q}$ and $\widetilde{g}\widetilde{g}$ production, there would be additional combinatoric possibilities or else one would need to implement a selection criterion for choosing the jets that one hoped came from $\widetilde{q}$ decays directly.

# Previous LHC Work

No time for a proper summary, but here are the bottom lines prior to our work.

- Without making use of total cross section information and/or distribution shapes, the best result that I have seen is that of Lester (Les Houches 2004) (see also the earlier work of Kawagoe, Nojiri, Polesello, hep-ph/0312317, hep-ph/0410160), who uses the one-chain, $4$-visible particle approach with

$$\widetilde{g} \to \widetilde{b}b \to \widetilde{\chi}_2^0 bb \to \widetilde{l}lbb \to \widetilde{\chi}_1^0 llbb \tag{2}$$

with

$$m_{\widetilde{g}} = 650, \quad m_{\widetilde{b}} = 500, \quad m_{\widetilde{\chi}_2^0} = 300, \quad m_{\widetilde{l}} = 200, \quad m_{\widetilde{\chi}_1^0} = 150 \tag{3}$$

and finds with $100$ events an error on $m_{\widetilde{\chi}_1^0}$ of $17\%$.

Mass differences have much smaller error.

I can't be sure, but I don't think this analysis included resonance width effects, which are actually quite important.

- **Analyses based on edges in various masses that can be reconstructed from visible particles in the chain give accurate results for mass differences, but allow a broad swath of possible absolute mass scales, $i.e.$ for $m_{\widetilde{\chi}_1^0}$, as already sketched.**

  **As well as the LHC/ILC report, see also A.J. Barr, C.G. Lester, M.A. Parker: hep-ph/050843.**

- **If the model is known and all branching ratios for the different chain decay sequences can be computed, then total cross sections and distribution shapes for different topologies can be used to determine the absolute scale.**

  **This, however, is rather model dependent, and even doing so still leaves discrete ambiguities for the absolute scale.**

  - **One, and probably the best, such analysis was that of Gjeltsen, Miller, Osland: hep-ph/0410303.**
    **The cases they analyzed were a low-mass SPS1a-like scenario and a high-mass scenario along the SPS1a line with lower event rate.**
    **They confirm that without the use of distribution shapes the absolute mass scale is poorly determined.**
    **Using distribution shapes, in the low-mass SPS1a case, they found two**

discrete solutions. Within either possible solution $m_{\tilde{\chi}_1^0}$ can be determined to about $5\%$, but there was a $10$ GeV separation between the two discrete possibilities, one of which was centered on the correct value and the other of which was too low by about $10$ GeV.
In the high mass scenario, results were much worse.

– As well as reconfirming the fact that edges only give mass differences, A.J. Barr, C.G. Lester, M.A. Parker: hep-ph/050843 looked at how well the absolute mass scale could be determined using a $10\%$ measurement of the cross section, assuming that the model was already known ($i.e.$ including decay chain, branching ratios, relative rates for sparticle pair production and so forth).
They found an error on $m_{\tilde{\chi}_1^0}$ of order $15 - 20$ GeV.

- Clearly, one would like to use pure kinematics to get the absolute masses, and further improve the accuracy to $10$ GeV or hopefully even better.

# 2 chains — 2 visible particles per chain

- **We claim that one can do well at the LHC by taking a more global point of view and using as much information as is available in every event.**

  **Our approach can be applied to many different types of event topologies, but here we focus on a subcomponent of the SPS1a type event in a way that has not been previously attempted.**

  **Consider the chain decay sequence:**

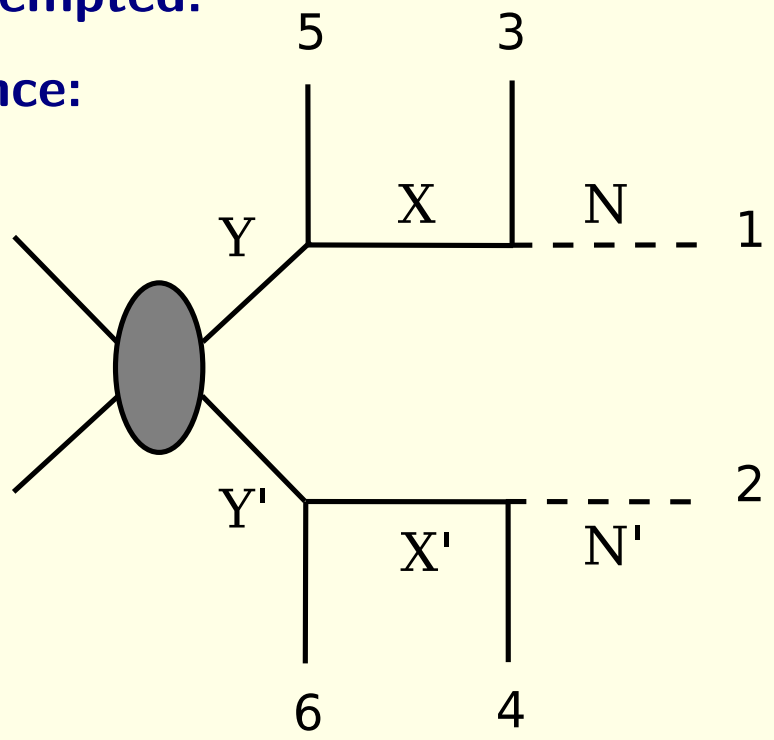


**Figure 6:** *A typical chain decay topology.*

**Note: some cuts to isolate a given topology are required (just as in the previous analyzes) — perhaps OSET would do the job. By this, we don't mean perfect isolation — roughly a ratio of $S/B > 2$ is certain to work, where $B$ could include old physics and new physics signals of other topologies. Even $S/B \sim 1$ is probably workable.**

**This topology can be applied to many processes with 4 visible and 2 invisible particles.**

**For example, suppose $M_Y = M_{Y'}$, $M_X = M_{X'}$, and $M_N = M_{N'}$.**

**Examples that fit this:**

$$
\begin{aligned}
t\bar{t} &\rightarrow bW^+bW^- \rightarrow bl^+\nu bl^-\bar{\nu} \\
\tilde{\chi}_2^0\tilde{\chi}_2^0 &\rightarrow l\tilde{l}l\tilde{l} \rightarrow ll\tilde{\chi}_1^0ll\tilde{\chi}_1^0 \\
\tilde{q}\tilde{q} &\rightarrow q\tilde{\chi}_2^0q\tilde{\chi}_2^0 \rightarrow ql\tilde{l}ql\tilde{l} \rightarrow qll\tilde{\chi}_1^0qll\tilde{\chi}_1^0 \\
\tilde{t}\bar{\tilde{t}} &\rightarrow b\tilde{\chi}^+\bar{b}\tilde{\chi}^- \rightarrow bW^+\tilde{\chi}_1^0\bar{b}W^-\tilde{\chi}_1^0
\end{aligned}
$$

**The third entry above is the SPS1a' case of interest.**

Let us count the constraints and unknowns once again. For this we (temporarily) assume that the particles are exactly on-shell and that experimental resolutions are perfect.

1. There are $8$ unknowns corresponding to the $4$-momenta of the $N$ and $N'$.

2. There are $2$ constraints on these coming from knowledge of the visible transverse momenta. (We are assuming that the longitudinal momentum and energy of the collision is not known, as appropriate at a hadron collider.)

   If there are extra visible jets in the event we just include them in visible $\vec{p}_T$.

   The visible particles $3$, $4$, $5$ and $6$ need not be stable. We just need to be able to determine their $4$-momenta (e.g. $W \to jj$ is ok but $W \to \ell\nu$ is not).

3. There are the $3$ constraints coming from requiring the equalities: $M_Y = M_{Y'}$, $M_X = M_{X'}$, and $M_N = M_{N'}$.

4. Thus, for each event, since $(8-2)-3=3$ we see that if we know the $3$ masses, then we can solve for the $4$-momenta of the $N$ and $N'$ and vice versa.

The equations are quartic, and so there can be $4$, $2$ or $0$ solutions (with acceptable positive real energies for the $N$ and $N'$). If not $0$, then the event is "solved" for those particular mass choices.

5. For each event, we scan through the mass space to see if one or more of the discrete solutions is acceptable.

   Each event then defines a $3$-dimensional region in the $3$-dimensional mass space that is physically acceptable.

6. As we increase the number of events the $3$-dimensional mass region consistent with all events becomes smaller.

   However, in general (and in practice) this region will not shrink to a point.

   Thus, we need additional methods to pick out the correct point in mass space.

- To illustrate our approach, we can consider the explicit example

$$\widetilde{\chi}_2^0\widetilde{\chi}_2^0 \to \ell\widetilde{\ell}\ell\widetilde{\ell} \to \ell\ell\widetilde{\chi}_1^0\ell\ell\widetilde{\chi}_1^0 \quad ,$$
$$i.e. \quad Y = Y' = \widetilde{\chi}_2^0, \quad X = X' = \widetilde{\ell}, \quad N = N' = \widetilde{\chi}_1^0 \, ,$$

**which we generate as a subcomponent of**

$$\widetilde{q}\widetilde{q} \to q\widetilde{\chi}_2^0 q\widetilde{\chi}_2^0 \to \ldots \to q\ell\ell\widetilde{\chi}_1^0 q\ell\ell\widetilde{\chi}_1^0 \,. \tag{4}$$

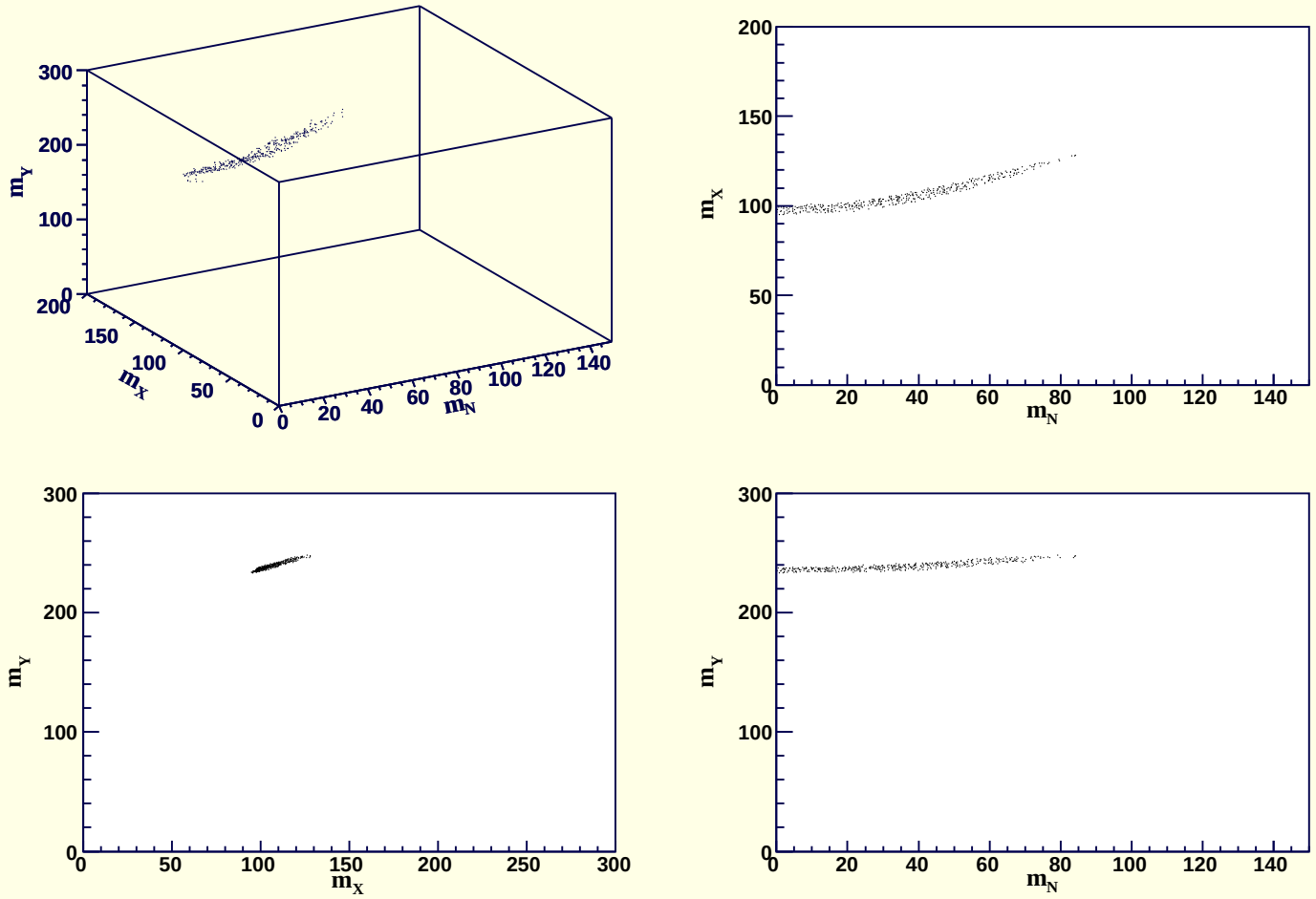


**Figure 7:** *Mass region (in GeV) that can solve all events.* $\mathbf{500}$ *generated events for* $m_Y = 246.6$ GeV, $m_X = 128.4$ GeV *and* $m_N = 85.3$ GeV, *using correct chain assignments and perfect resolution. Masses from 'Model I', with large* $m_{\widetilde{\chi}_2^0}$.

**We found that the correct masses lie at the end point of the allowed region. A graphical picture is:**

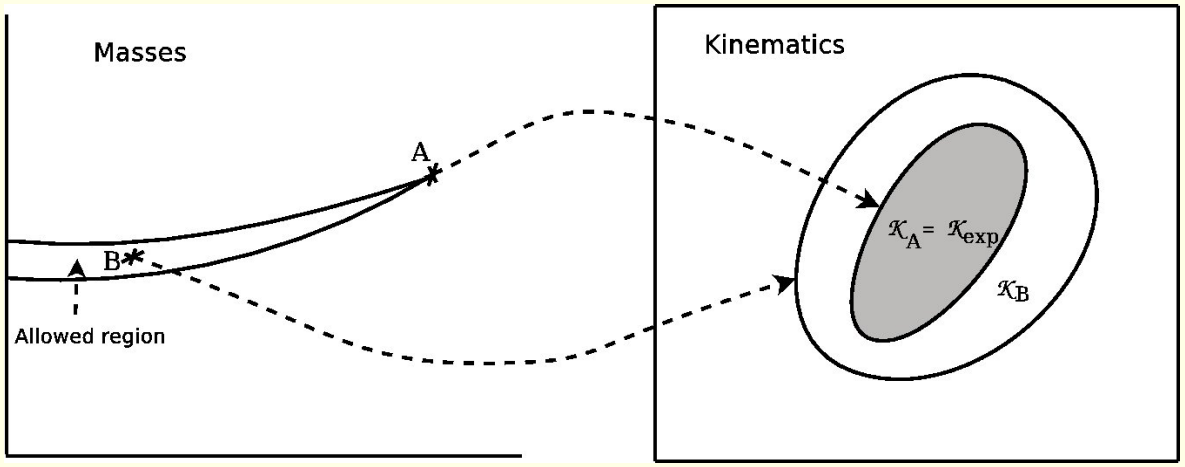


**Figure 8:** *Map between mass space and kinematic space. The nominal masses, point $A$, produces a kinematic region that coincides with the experimental region: $\mathcal{K}_A = \mathcal{K}_{exp}$. A point $B$ inside the allowed mass region produces a larger kinematic region: $\mathcal{K}_B \supset \mathcal{K}_{exp}$.*

**The kinematic space $\mathcal{K}$ refers to the set of observable momenta of the 4 leptons in the chain.**

**The allowed masses in $\mathcal{M}$ space are those for which every point in the $\mathcal{K}_{exp}$ part of $\mathcal{K}$ space produces at least one acceptable set of $\vec{p}_N$ and $\vec{p}_{N'}$, $i.e.$ is 'solved'.**

a) The correct set of masses, $\mathcal{M}$ at point $A$ in Fig. 8, produces a kinematic region $\mathcal{K}_A$ that coincides with the experimental one, $\mathcal{K}_A = \mathcal{K}_{exp}$, as long as the experimental statistics is large enough.

b) A different mass point produces a region that is either smaller or larger than $\mathcal{K}_{exp}$[1].

c) If smaller, the mass point does not appear in the mass region for which **all** events are solved.

d) If larger, all events are solved; we denote this kind of point, with mass set $\mathcal{M}'$, as point $B$ in Fig. 8.

e) Let us shift the masses slightly to $\mathcal{M}' + \delta\mathcal{M}'$.

- If the kinematic region for which we have acceptable solutions still covers $\mathcal{K}_{exp}$, then $\mathcal{M}' + \delta\mathcal{M}'$ is still within the allowed region.
- Apparently, point $B$, which produces a region larger than $K_{exp}$, has the freedom to move in all directions and must live inside the allowed region.
- On the other hand, the correct mass point $A$, which produces exactly $\mathcal{K}_{exp}$, has the least freedom to move and must be located at an end point of the allowed region.

**However,** with finite resolutions and combinatorics (which lepton goes where

[1] In general cases, there could exist degenerate points that produce exactly the same kinematic region as the correct one. It is impossible to raise the degeneracy using pure kinematics.

**in the two chains), not all events can be solved by the correct mass point.**

**$\Rightarrow$ The correct mass point will not lie within the intersection region (assuming there is any such region left).**

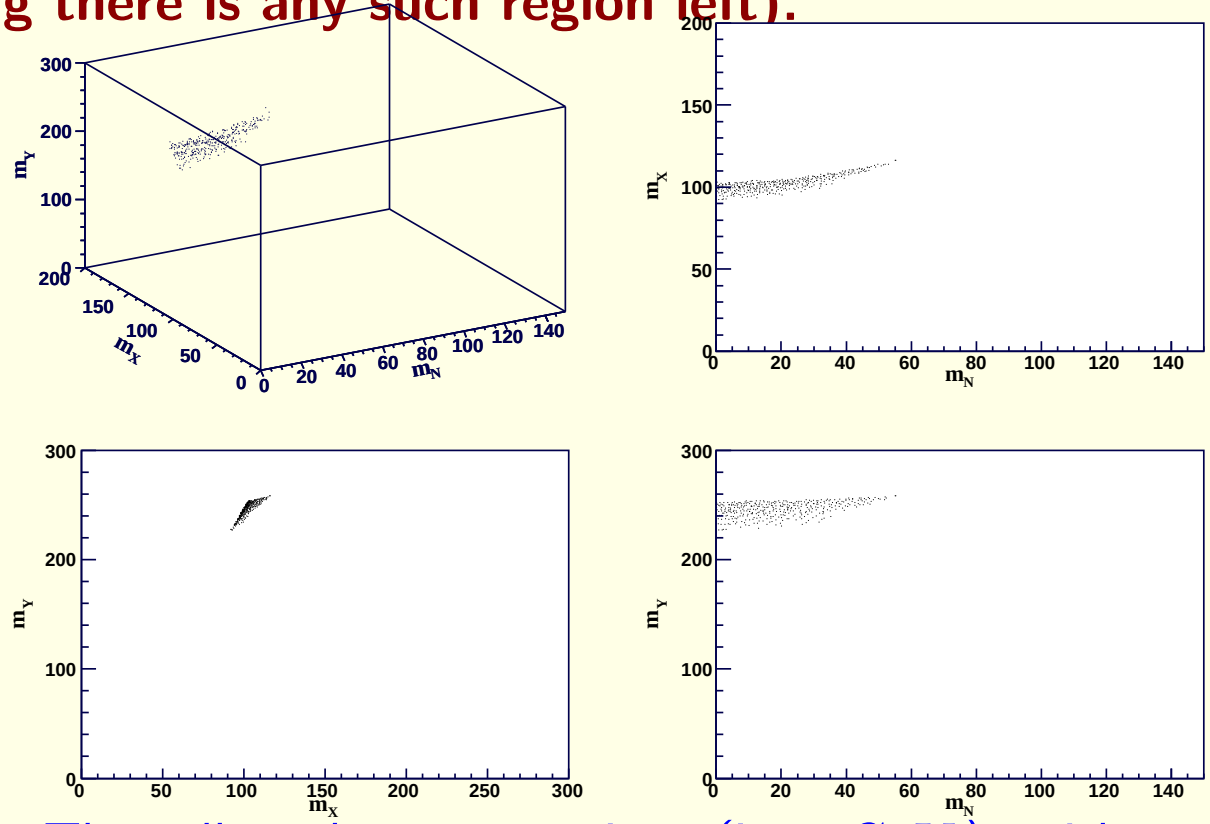


**Figure 9:** *The allowed mass region (in* $\mathrm{GeV}$*) with smearing (ALTFAST) and wrong combinatorics.* $\mathbf{500}$ *generated events for Model I masses:* $m_Y = 246.6\ \mathrm{GeV}, m_X = 128.4\ \mathrm{GeV}$ *and* $m_N = 85.3\ \mathrm{GeV}$*. Cuts:* $|\eta| < 2.5$*,* $p_T(\ell) > 6\ \mathrm{GeV}$*.*

- **In the more realistic case, the correct mass choices do not correspond to**

an endpoint but rather correspond to the choices such that changes in the masses result in the most rapid decline in the number of solved/consistent events.

- Looking for this point of steepest decline in a $3$-dimensional space is numerically difficult.

- If we fix two of the masses, and vary the $3rd$ mass, then we can usually identify the point at which the number of solved events starts a steep decline as this $3rd$ mass is changed.

  This will allow an iterative approach.

- The approach that works is to cycle through the $3rd$-mass choices, $m_N$, $m_X$ and $m_Y$ in that order, and at each stage look for the peak in the number of solved/consistent events as a function of the $m_N$ mass each time it is the $3rd$-mass. Then, update this $3rd$-mass to the peak location.

  The 'peaks' are actually obtained by the intersection of the two fitted straight lines illustrated in the following figure, where two masses are set to their correct values and the $3rd$-mass is varied.

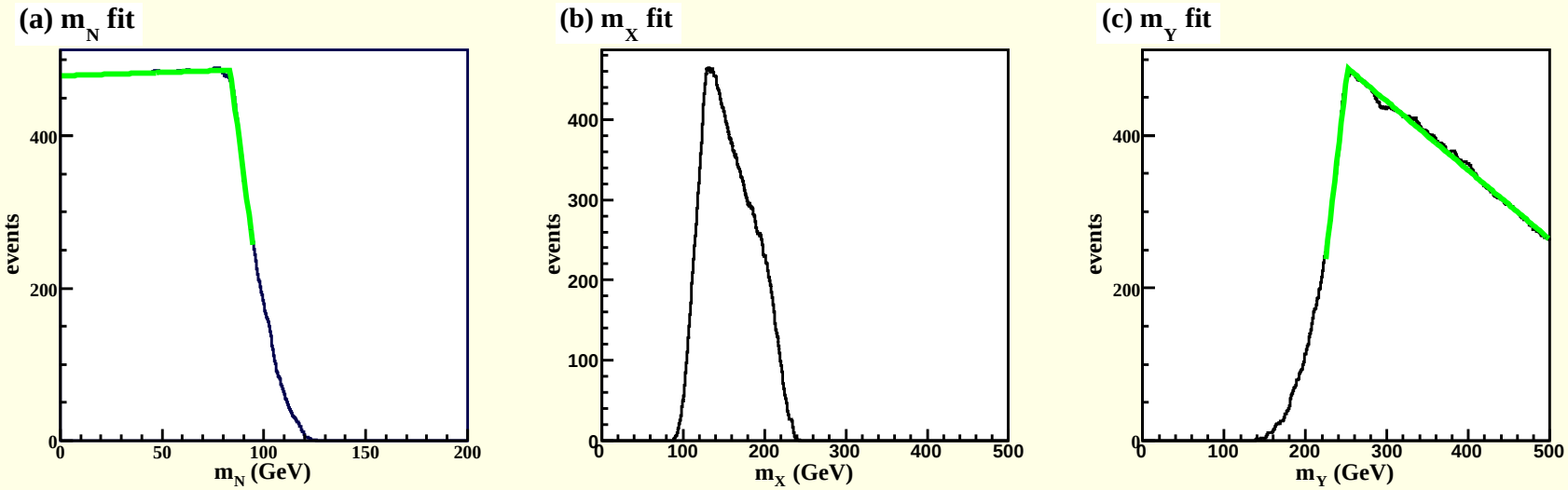


**Figure 10:** *One-dimensional fits by fixing the other two masses at the correct values. 500 events, combinatorics, smearing and simple cuts included. Peaks are close to correct masses.*

- **We now get more realistic. For certain soft-SUSY parameters one obtains our Model I with**

$$m_{\tilde{g}} \sim 524, \quad m_{\tilde{d}_L,\tilde{s}_L} \sim 438, \quad m_{\tilde{u}_L,\tilde{c}_L} \sim 431$$
$$m_{\tilde{\chi}_2^0} \sim 246.6, \quad m_{\tilde{\mu}_R} \sim 128.4, \quad m_{\tilde{\chi}_1^0} \sim 85.3 \qquad (5)$$

For this point, the net cross section available is

$$\sigma\left(pp \to \sum_{q,q'=u,d,c,s} \widetilde{q}_L\,\widetilde{q}'_L + \sum_{q,q'=u,d,c,s} \widetilde{q}_L\,\overline{\widetilde{q}'_L} + \sum_{q,q'=u,d,c,s} \overline{\widetilde{q}_L}\,\overline{\widetilde{q}'_L}\right) \sim 2.9 \times 10^4 \text{ fb}\,, \tag{6}$$

coming from all sources including $gg$ fusion, $u_L u_L$ fusion, *etc.* The branching ratios relevant to the particular decay chain we examine are

$$\begin{aligned} B(\widetilde{q}_L \to q\widetilde{\chi}_2^0) &\sim 0.27 \quad (q = u, d, c, s) \\ B(\widetilde{\chi}_2^0 \to \widetilde{\mu}_R^{\pm}\mu^{\mp}) &\sim 0.124 \\ B(\widetilde{\mu}_R^{\pm} \to \mu^{\pm}\widetilde{\chi}_1^0) &= 1\,. \end{aligned} \tag{7}$$

The net effective branching ratio for the double decay chain is

$$B(\widetilde{q}_L\widetilde{q}_L \to 4\mu\widetilde{\chi}_1^0\widetilde{\chi}_1^0) \sim (0.27)^2 \times (0.124)^2 \sim 1.12 \times 10^{-3} \tag{8}$$

for any one $\widetilde{q}_L$ choice. The effective cross section for the $4\mu\widetilde{\chi}_1^0\widetilde{\chi}_1^0$ final state is then

$$\sigma(4\mu\widetilde{\chi}_1^0\widetilde{\chi}_1^0) \sim 2.9 \times 10^4 \text{ fb} \times 1.12 \times 10^{-3} \sim 32.5 \text{ fb}\,. \tag{9}$$

For an integrated luminosity of $L = 90$ fb$^{-1}$, this gives us 2900 $4\mu\widetilde{\chi}_1^0\widetilde{\chi}_1^0$ events before any cuts are applied.

Initial and final state radiation, resonance widths, combinatorics and experimental resolutions (as in ATLFAST) are all included.

To reduce the SM background, we require that all muons are isolated and pass the kinematic cuts:

$$|\eta|_\mu < 2.5, \quad P_{T\mu} > 10 \text{ GeV}, \quad \not{p}_T > 50 \text{ GeV}. \tag{10}$$

With these cuts, the four-muon SM background is negligible.

The number of signal events is reduced from 2900 to about 1900.

The procedure comprises the following steps:

1. Randomly select masses $m_Y > m_X > m_N$ that are below the correct masses (for example, the current experimental limits).
2. Plot the number of solved events, $N_{evt}$, as a function of one of the 3 masses in the recursive order $m_N$, $m_X$, $m_Y$ with the other two masses fixed. In the case of $m_Y$ and $m_N$, we fit $N_{evt}$ for the plot with two straight lines and adopt the mass value at the intersection point as the updated mass. In the case of $m_X$, the updated mass is taken to be the mass at the peak of the $N_{evt}$ plot.

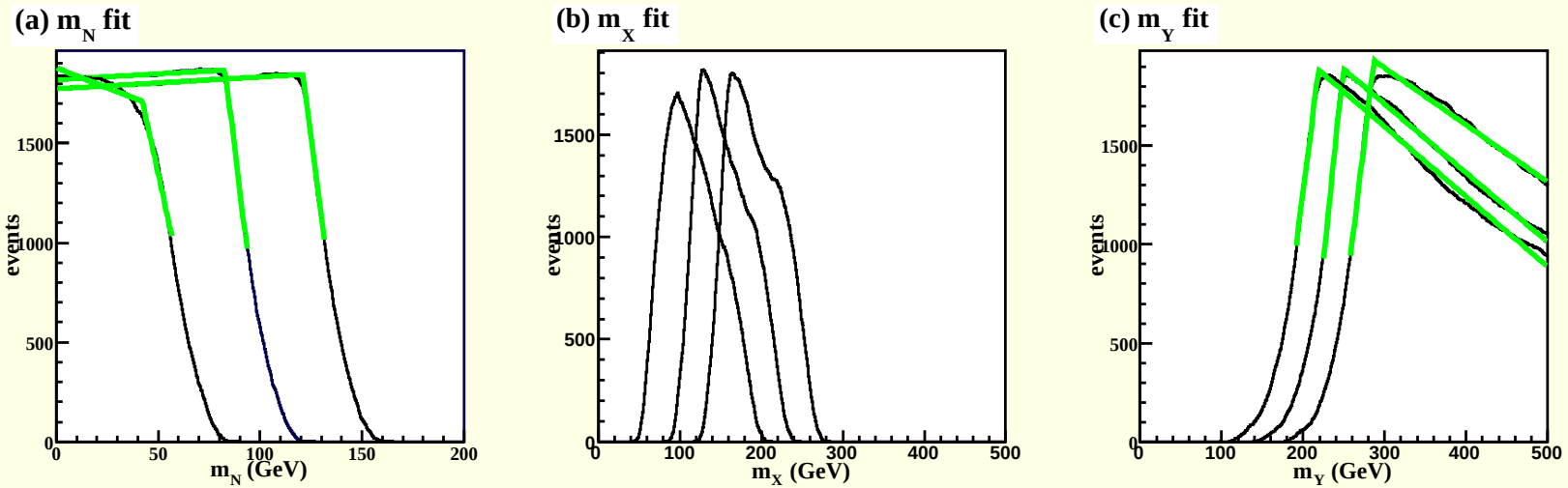


**Figure 11:** *A few steps showing the migration of the one dimensional fits. The middle curve in each plot corresponds to masses close to the correct values.*

**A few intermediate one-dimensional fits are shown in Fig. 11.**

3. **Each time after a fit to $m_N$, record the number of events at the intersection (sometimes called the turning point) of the two straight lines, as exemplified in Fig. 11 a. This event number at the turning point will in general be non-integer.**
4. **Repeat steps 2 and 3. The number of events recorded in step 3 will in general increase at the beginning and then decrease after some steps, as seen in Fig. 12. Halt the recursive procedure when the number of (fitted) events has sufficiently passed the maximum position.**
5. **Fit Fig. 12 to a (quartic) polynomial and take the position where the polynomial is maximum as the estimated $m_N$.**
6. **Keep $m_N$ fixed at the value in step 5 and do a few one-dimensional fits**

for $m_Y$ and $m_X$ until they are stabilized. Take the final values as the estimates for $m_Y$ and $m_X$.

- The end result is the plot below.

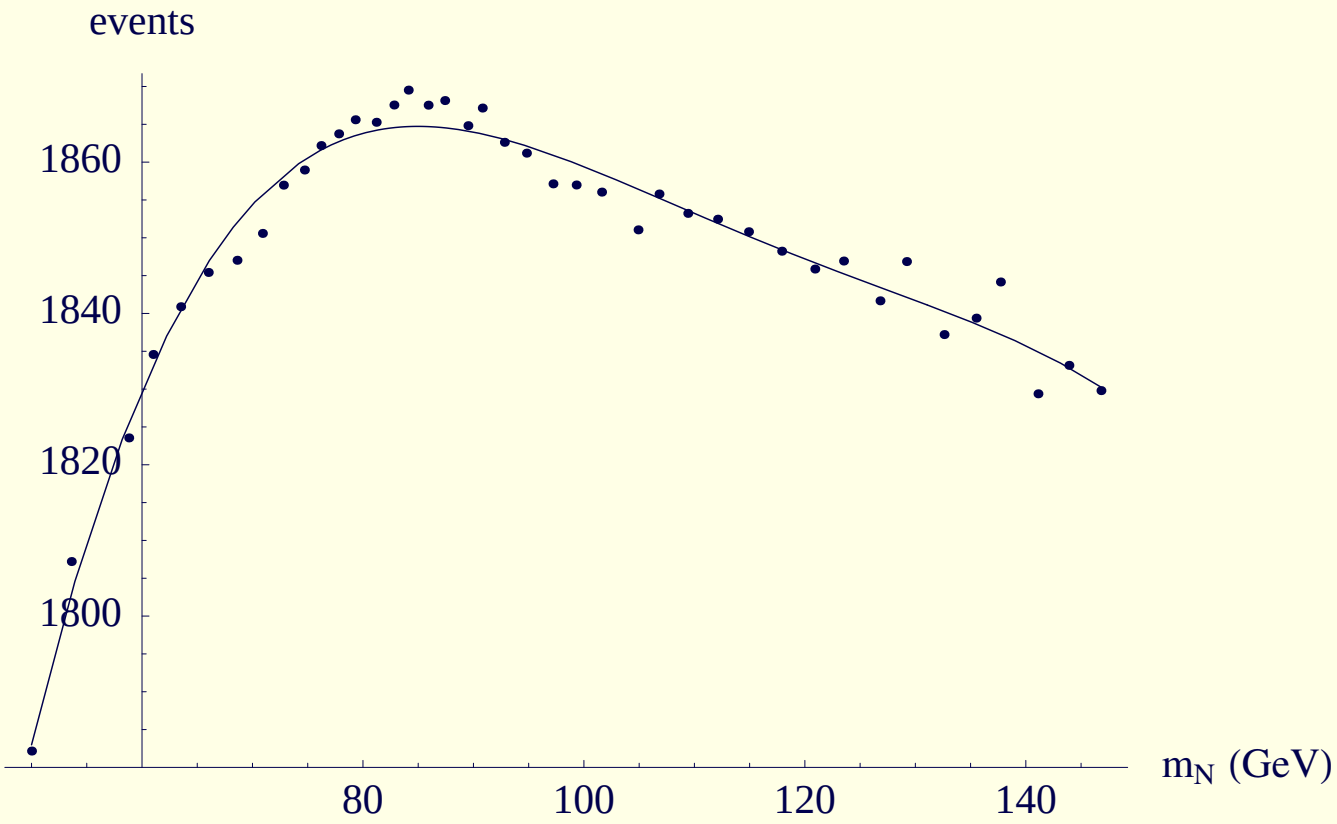


**Figure 12:** *The final plot for determining $m_N$. The position of the maximum of the fitted polynomial is taken to be the estimation of $m_N$..*

Remarkably, the point at which the turnover occurs gives $M_N$ ($and$ $M_X$

and $M_Y$) to good accuracy.

The final values for the masses in one "experiment" were determined as

$$\{252.2, 130.4, 85.0\}\ \mathrm{GeV} \quad vs. \quad \{246.6, 128.4, 85.3\}\ \mathrm{GeV} \tag{11}$$

Remarkably, the $N$ mass is extremely accurate and the $Y$ mass quite close as well.

A deeper understanding of our procedure can be gained by examining the graphical representation of the steps taken in the $(m_Y, m_N)$ plane shown in Fig. 13.

There, we display contours of the number of (fitted) events after maximizing over possible $m_X$ choices.

There is a 'cliff' of falloff in the number of solved events beyond about 1825 events. It is the location where this cliff is steepest that is close to the input masses, which are indicated by the (red) star.

The mass obtained by our recursive fitting procedure is indicated by the (blue) cross.

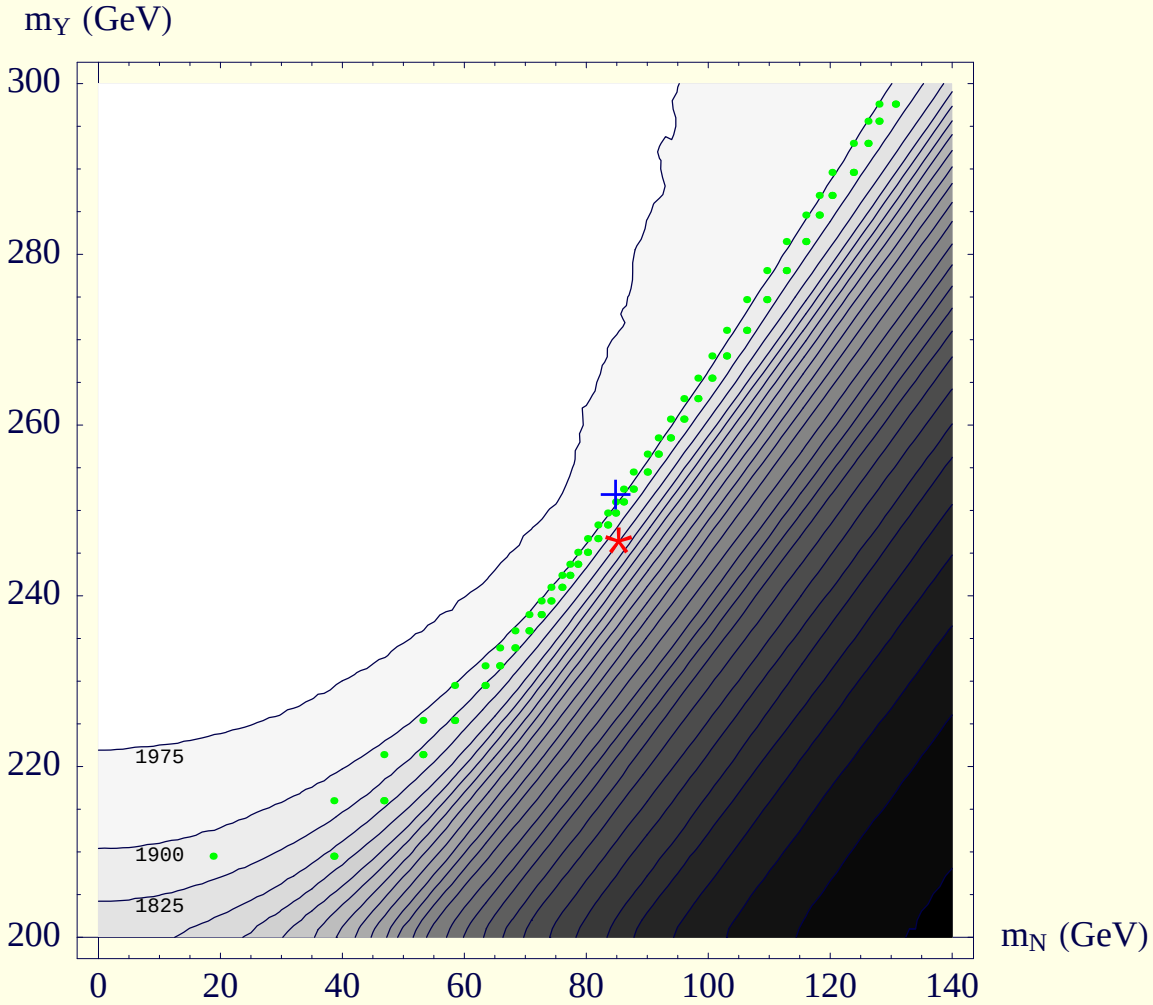


**Figure 13:** *Contours for the number of solved events in the $m_N \sim m_Y$ plane with 2000 events. The number of events is the maximum value obtained after varying $m_X$. Contours are plotted at intervals of 75 events, beginning with a maximum value of 1975. The green dots correspond to a set of one-dimensional fits. The ⋆ shows the input masses and the + shows our fitted masses.*

- **Error evaluation:**

**Must adopt an 'experimental' approach for such an empirical procedure:**

**Generate 10 different $90\ \mathrm{fb}^{-1}$ data samples and apply the procedure to each sample.**

**Estimate the errors of our method by examining the statistical variations of the 10 samples, which yields**

$$m_Y = 252.2 \pm 4.3\text{GeV}, \quad m_X = 130.4 \pm 4.3\text{GeV}, \quad m_N = 86.2 \pm 4.3\text{GeV}. \tag{12}$$

**The statistical variations for the mass differences are much smaller:**

$$\Delta m_{YX} = 119.8 \pm 1.0\text{GeV}, \quad \Delta m_{XN} = 46.4 \pm 0.7\text{GeV}. \tag{13}$$

**Compared with the correct values $\mathcal{M}_A = \{246.6, 128.4, 85.3\}$, we observe small biases in the mass determination, which means that our method has some "systematic errors".**

**However, these systematic errors are determined once we fix the experimental resolutions, the kinematic cuts and the fit procedure.**

Therefore, they can be easily corrected for, which leaves us errors for the absolute mass scale of $\sim$ *few* GeV and for the mass differences of $\sim 1$ GeV.

- **Backgrounds**

In the above example, the background is negligible with the applied cuts.

However, if in some other case the backgrounds turned out to be substantial, they could decrease the accuracy of the mass determination.

Instead of analyzing another process with sizable backgrounds, we stick to the four muon events studied above but make up more "backgrounds".

In particular, we consider the 4-muon events from top pair production, but unlike above we do not require the muons to be isolated (which eliminates this background).

$\Rightarrow$ a significant number of events have 4 hard muons.

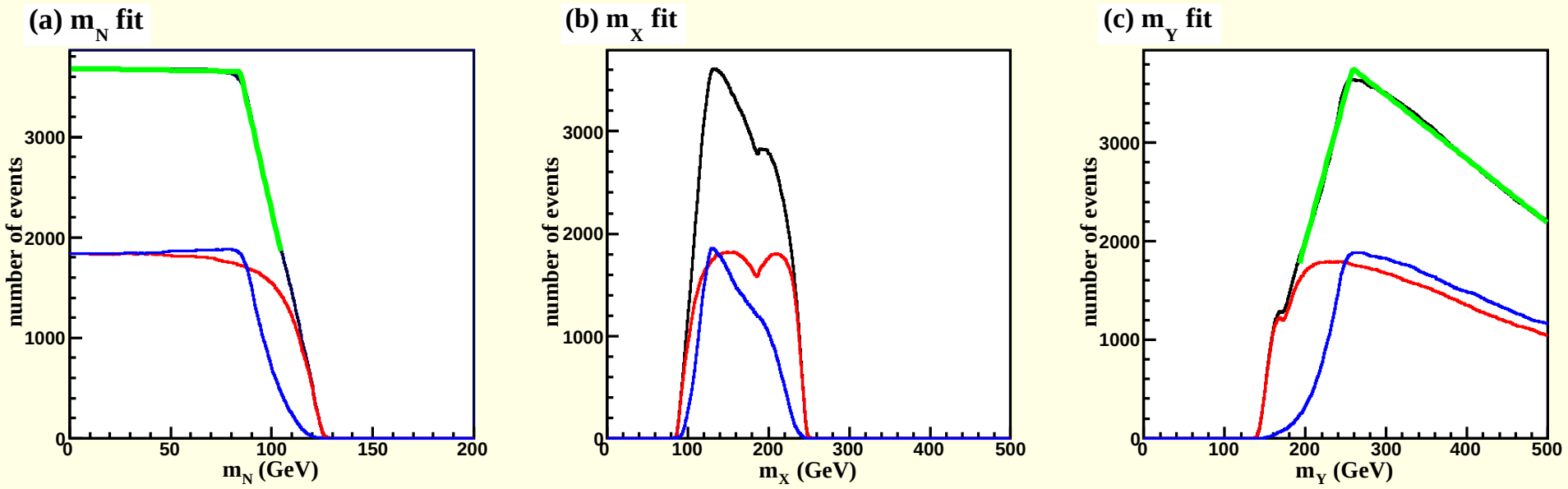


**Figure 14:** *Fits with $90 fb^{-1}$ signal events and an equal number of background events. Separate numbers of signal (blue) and background (red) events are also shown.*

**Adding an equal number of background events to $90 fb^{-1}$ signal events, we repeat the one-dimensional fits. A typical cycle around the correct masses is shown in Fig. 14.**

**For comparison the number of solvable signal events and background events are also shown separately.**

**The effect of background events is clear: the curve for solvable background**

events is much smoother around the turning point, and therefore smears but does not destroy the turning point.

Although we are considering one specific background process, this effect should be generic, unless the backgrounds happen to have non-trivial features around the turning points.

Nevertheless, due to the fact that there are 8 possible combinations, the chance that a background event gets solutions is quite large and they do affect the errors and biases of the mass determination.

This can be seen in Fig. 15, in which we have used the same 10 sets of signal events as in the previous subsection, but varied the number of background events according to the ratio $background/signal = 0, 0.1, 0.2, 0.5, 1$.

We observe increases in both the biases and variations.

But, if the backgrounds are understood (which if SM, they will be), then we can correct for them.

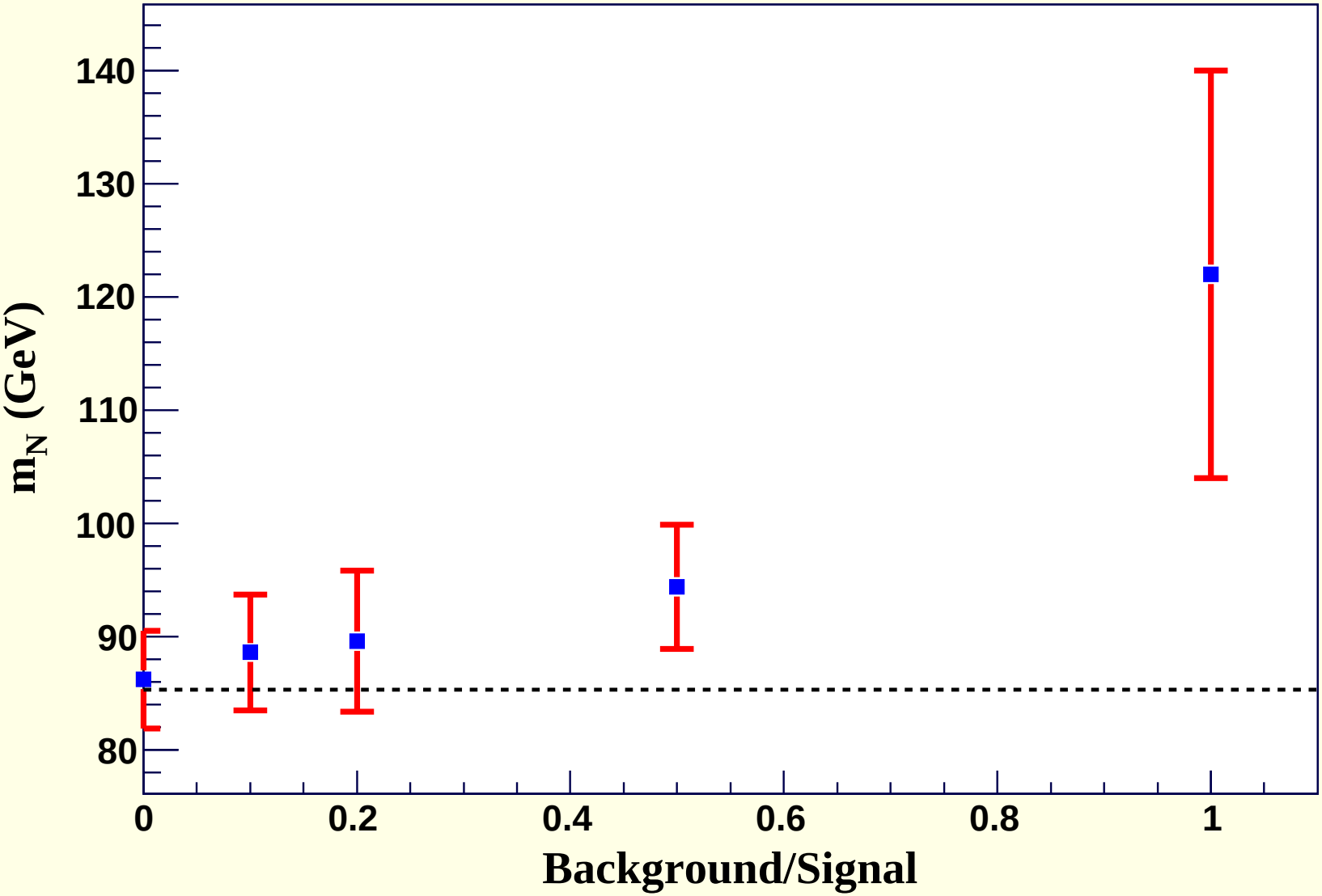


**Figure 15:** *$m_N$ determination with different background-signal ratio. The dashed horizontal line corresponds to the correct $m_N$.*

- **If it should be that $m_N \sim 0$, then we will know it.**

  **We have found that it would quickly become apparent that we were not finding a maximum in the included event number as $m_N$ is increased.**

  **We would then backtrack to $m_N = 0$ and find that actually the number of included events is largest there and declines as $m_N$ increases. A typical plot is shown in Fig. 16.**

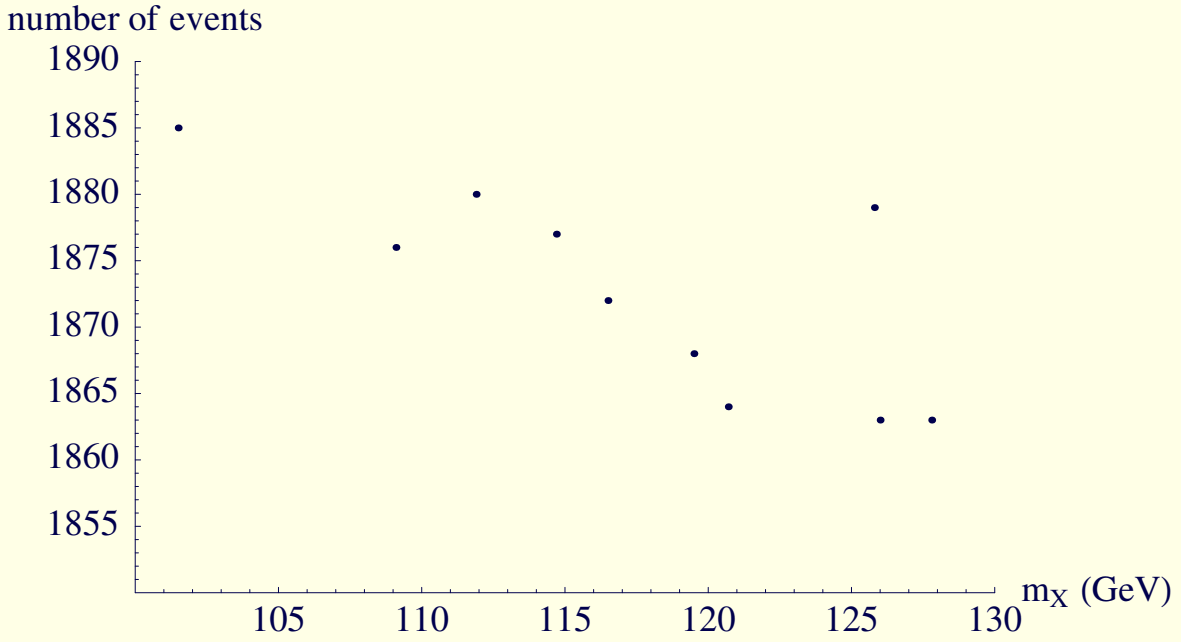


**Figure 16:** *$m_N$ determination for a case with $m_Y = 199.4$ GeV, $m_X = 100$ GeV and $m_N = 0.1$ GeV. Requires very large $\mu$ in SUSY model. 2000 event sample.*

- **Peculiar mass separation choices can give some special features.**

  **We are currently working on optimizing our procedures for such cases.**

- **We are confident that the experimental groups will actually end up doing even better in the end.**

  **In particular, if they understand the backgrounds then they can separately apply our procedure to them and subtract the background from the summed curves of Fig. 14, returning us to a situation close to the zero-background case first considered.**

**The SPS1a Point**

- **It is desirable to compare directly to the results obtained by others for the SPS1a SUSY parameter point.**

- **We perform the analysis using the same $4\mu\widetilde{\chi}_1^0\widetilde{\chi}_1^0$ final state that we have been considering. For the usual SPS1a mSUGRA inputs the masses for $Y = \widetilde{\chi}_2^0$, $X = \widetilde{\mu}_R$ and $N = \widetilde{\chi}_1^0$ (from ISAJET 7.75) are $180.3$ GeV, $142.5$ GeV and $97.4$ GeV, respectively.**

- This is a more difficult case than Point I considered earlier due to the fact that the dominant decay of the $\widetilde{\chi}_2^0$ is $\widetilde{\chi}_2^0 \to \tau\widetilde{\tau}_1$. The branching ratio for $\widetilde{\chi}_2^0 \to \mu\widetilde{\mu}_R$ is such as to leave only about $1200$ events in the $4\mu\widetilde{\chi}_1^0\widetilde{\chi}_1^0$ final state after $L = 300\ \mathrm{fb}^{-1}$ of accumulated luminosity.

- Cuts reduce the number of events further to $\sim 425$.

  This is too few for our technique to be as successful as for the earlier considered cases.

- After including combinatorics and resolution we obtain:

$$m_Y = 188 \pm 12\ \mathrm{GeV}\,, \quad m_X = 151 \pm 14\ \mathrm{GeV}\,, \quad m_N = 100 \pm 13\ \mathrm{GeV}\,. \tag{14}$$

  In Fig. 17, we give an SPS1a plot analogous to Fig. 12.

  Errors are determined by generating many such plots for different samples of $\sim 425$ events (the exact number changes depending upon event details).

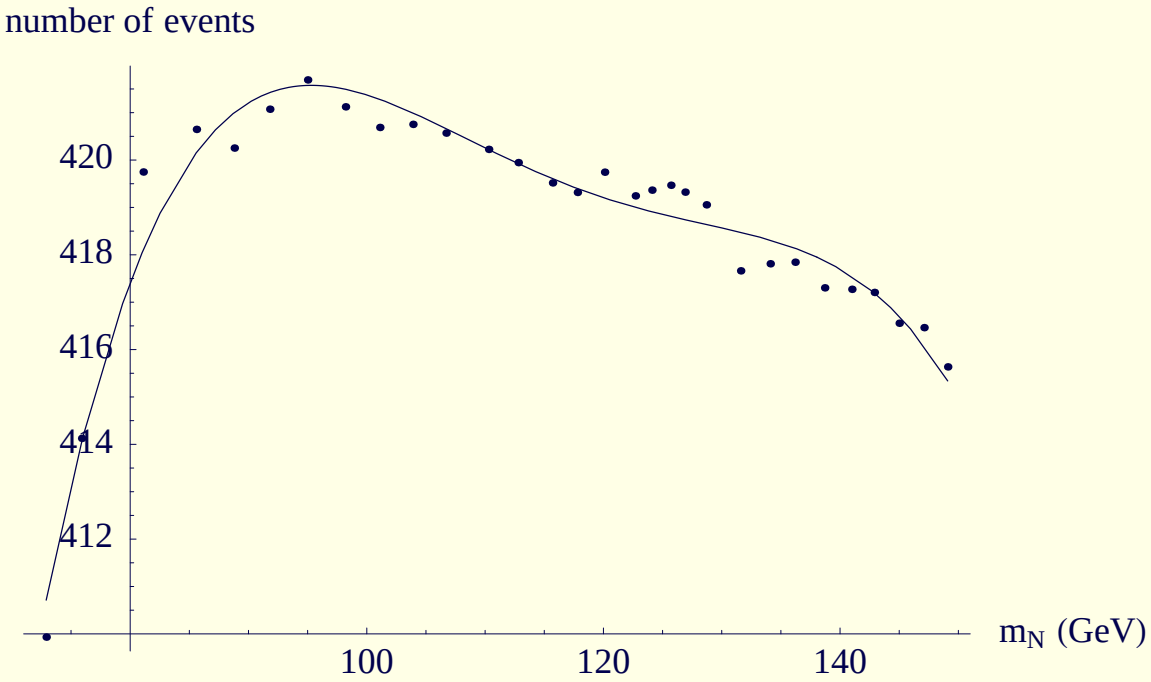


**Figure 17:** *Fitted number of events at the turning point as a function of* $m_N$ *for the fits for the SPS1a case.*

**Note the vertical scale. The change in the number of events as one varies** $m_N$ **is quite small for small event samples and this is what leads to the larger errors in this case.**

- **In principle, we must also take into account the fact that the dominant** $\widetilde{\chi}_2^0 \to \tau\widetilde{\tau}_1$ **decays provide a background to the purely muonic final state.**

**The background level (after cuts and branching ratios) is at about the $50\%$ level. However, using other channels involving $e$'s to which it, but not our signal, contributes, we can subtract this background statistically.**

**We have not yet performed the relevant procedure to see how well we do, but we expect that the net background contamination will be equivalent to $B/S \lesssim 0.1$, a level for which our techniques work very well and the errors quoted earlier for the SPS1a point will not be increased by very much.**

# 2 chains: 3 visible particles per chain

- Recall from the counting section that to solve requires just $n = 2$ events.

  There are many ways to set up the equations. The most convenient form leads (for 2 events) to 3 simultaneous quadratic equations.

  There are multiple solutions to these equations for any 2 events, even before including combinatorics and resolution.

  However, before combinatorics and resolutions, typically only one of the multiple solutions is common to all pairs of events that one can consider.

  It is easy to get lots of pairs of events; for example, 58 events leads to 1653 pairs.

  We again focus on the decay chain $\tilde{q} \to q\tilde{\chi}_2^0 \to q\mu\tilde{\mu}_R \to \tilde{\chi}_1^0 q\mu\mu$ with SPS1a masses $m_{\tilde{q}} = 565$ GeV, $m_{\tilde{\chi}_2^0} = 180$ GeV, $m_{\tilde{\mu}_R} = 142$ GeV and $m_{\tilde{\chi}_1^0} = 97$ GeV.

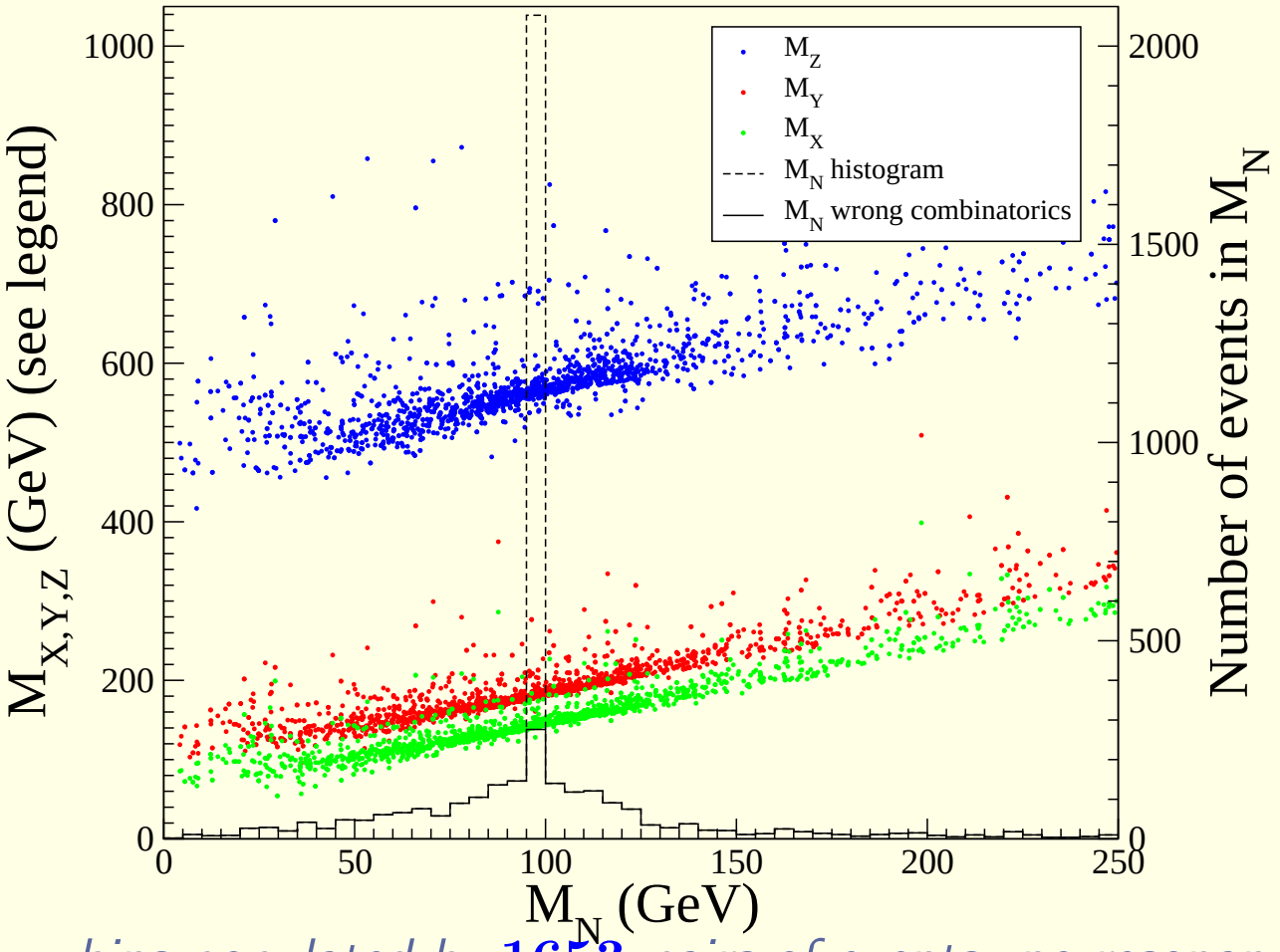


**Figure 18:** *$m_N$ bins populated by* **1653** *pairs of events: no resonance width effects are included, all squarks are taken degenerate and no resolution effects are included, but correct combinatoric uncertainties are and give the "pedestal".*

**In the above plot, you see the ideal situation: narrow width approximation for all the intermediate states; exactly degenerate squark masses (vs. the real SPS1a masses that have some differences between 1st two generations); and no resolution smearing —only combinatoric reassignments are incorporated.**

**To be more realistic, one should do the following;**

1. **generate $\widetilde{q}_L\widetilde{q}_L$ production with ISR and FSR jets turned on;**
2. **allow for squark mass differences — e.g. for SPS1a point, we find**

$$m_{\widetilde{u}_L} = m_{\widetilde{c}_L} = 565 \text{ GeV} \quad \text{vs.} \quad m_{\widetilde{d}_L} = m_{\widetilde{s}_L} = 571 \text{ GeV}\,. \tag{15}$$

3. **include the decay widths of the $\widetilde{q}_L$'s, $\widetilde{\chi}_2^0$'s, . . .**
4. **allow for combinatoric interchanges in which muons are placed in all physically possible places along the two decay chains;**
5. **allow for interchanging the two jets that we choose to associate with the primary $\widetilde{q}_L$ decays;**
   **(We choose these two jets by taking those with the largest $p_T$'s — sometimes this is not the correct choice.)**
6. **smear the momenta of the jets and muons using the resolutions of ATLFAST.**

**Note: When solving for consistent masses for all the particles at once, jet energy smearing, combinatorics and so forth will influence the masses extracted further down the chain for $\widetilde{\chi}_2^0, \ldots$.**

**$\Rightarrow$ the excellent $\mu$ momentum resolution will not help all that much.**

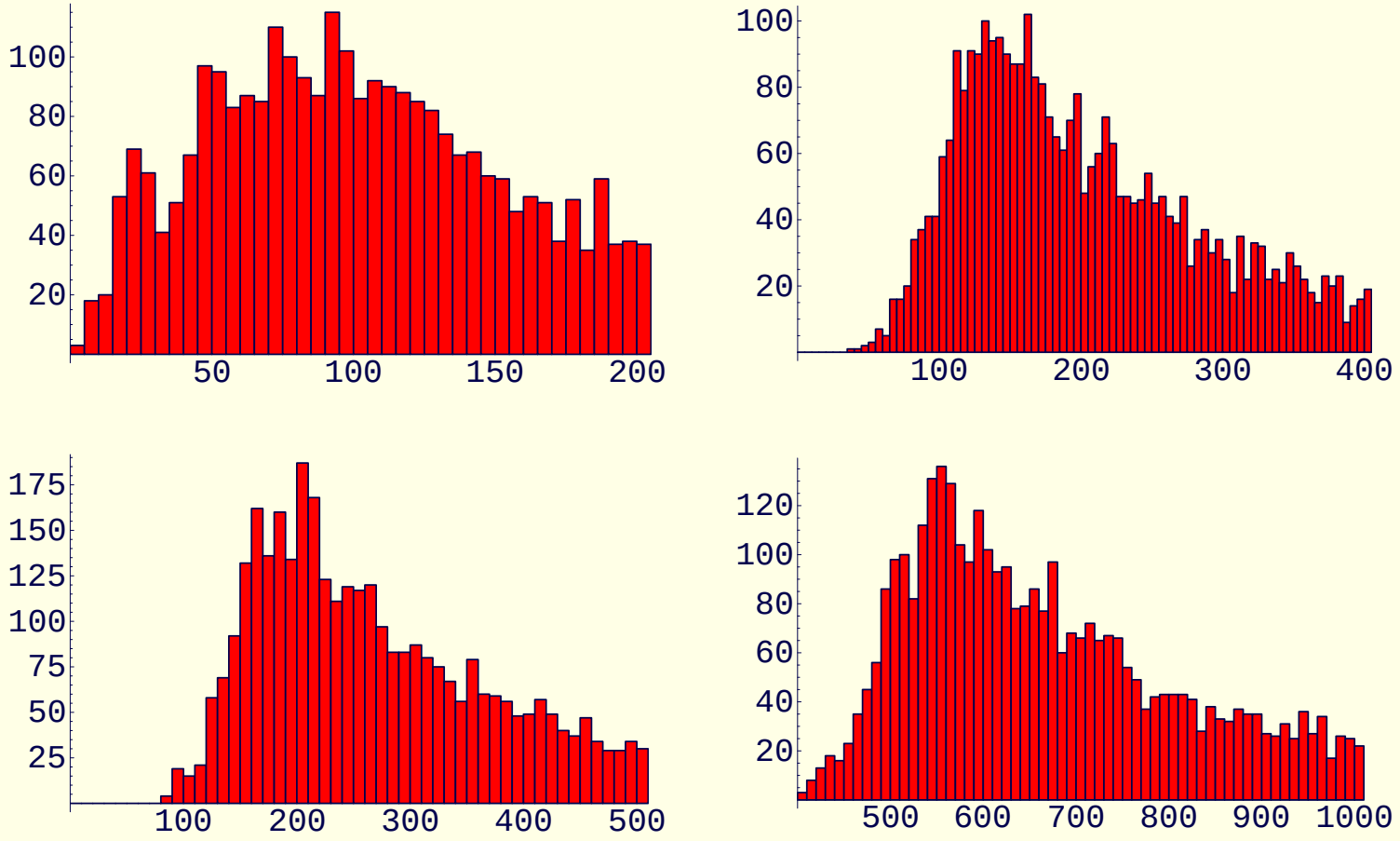


**Figure 19:** *Mass bins populated by* $\mathbf{120}$ *pairs of events:* resolution *effects are included,* combinatoric interchanges *are included, and* squark mass differences and resonance widths *are included.*

**Target SPS1a masses:** $m_{\widetilde{\chi}_1^0}, m_{\widetilde{\mu}_R}, m_{\widetilde{\chi}_2^0}, m_{\widetilde{q}} = \mathbf{97, 142, 180, 565}$ GeV. **Peaks are close to the actual masses. We are currently working on further refinements and error analyses,** $e.g.$ **by fitting to the peak of such distributions and using different sets of** $\mathbf{120}$ **pairs.**

# Conclusions

- **Using $2$ chains with $2$ visible particles each, $\Rightarrow \sim$ *few* GeV to $10$ GeV accuracy for the absolute mass scale is achievable at the LHC, depending upon the number of events available.**

- **Using more visible particles is likely to improve further on this result — refinement and error analysis of the case where we consider $2$ chains with $3$ visible particles in each chain is under way.**

  **Consequences:**

  1. **The above accuracy, even in the difficult SPS1a case, should be sufficient to eliminate the 'slider' degeneracies of the LHC inverse solutions.**
  2. **The accuracy already achieved will aid enormously in the GUT extrapolation.**
  3. **It will also greatly increase the accuracy of the dark matter calculation.**

- **The ability to get an absolute mass scale out of LHC data could be quite crucial for determining whether the ILC500 is sufficient or one needs to go to ILC1000.**

- **Our technique can, of course, be combined with the other techniques outlined at the beginning to obtain the best possible overall mass scale and mass differences.**

- **Don't forget that we must understand how to single out a single topology ($i.e.$ suppress others adequately) in the case that there are many new physics topologies.**

  **If this cannot be done, then we must learn how to work with multiple topologies. We believe our techniques can be generalized to such a situation.**